Two Distinct Modes of Processive Kinesin Movement in Mixtures of ATP and AMP-PNP

Radhika Subramanian and Jeff Gelles

Department of Biochemistry, Brandeis University, Waltham, MA 02454

An enzyme is frequently conceived of as having a single functional mechanism. This is particularly true for motor enzymes, where the necessity for tight coupling of mechanical and chemical cycles imposes rigid constraints on the reaction pathway. In mixtures of substrate (ATP) and an inhibitor (adenosine 5′-(β,γ-imido)triphosphate or AMP-PNP), single kinesin molecules move on microtubules in two distinct types of multiple-turnover "runs" that differ in their susceptibility to inhibition. Longer (less susceptible) runs are consistent with movement driven by the alternating-sites mechanism previously proposed for uninhibited kinesin. In contrast, kinesin molecules in shorter runs step with AMP-PNP continuously bound to one of the two active sites of the enzyme. Thus, in this mixture of substrate and inhibitor, kinesin can function as a motor enzyme using either of two distinct mechanisms. In one of these, the enzyme can accomplish high-duty-ratio processive movement without alternating-sites ATP hydrolysis.

The Journal of General Physiology

INTRODUCTION

Conventional kinesin (kinesin-1) is an ATPase that drives intracellular transport along microtubules. The enzyme moves parallel to microtubule protofilaments by making discrete 8-nm steps with each step tightly coupled to ATP hydrolysis (for review see Schief and Howard, 2001). The structure of a homodimeric kinesin construct crystallized in the presence of ADP reveals exactly two nucleotide binding sites, one in each subunit (Kozielski et al., 1997).

Kinesin moves processively, meaning that the enzyme can take multiple steps before dissociating from a microtubule. This movement has a duty ratio of ∼1, indicating that the enzyme spends essentially its entire catalytic cycle in states that allow neither dissociation from the microtubule nor free sliding along the microtubule axis. Certain one-headed kinesin homologues exhibit processive movement (Okada et al., 1995) as do some (Inoue et al., 2001) but not all (Berliner et al., 1995; Vale et al., 1996; Hancock and Howard, 1998; Young et al., 1998) artificial one-headed constructs of conventional kinesin. In contrast, high-duty-ratio movement appears to have an absolute requirement for two heads. It is natural to assume that catalytic activity of two heads is required to drive the conformational changes and modulation of head-microtubule affinity required for high-duty-ratio movement (Young et al., 1998). While motor enzymes (e.g., muscle myosin) that function in large assemblies can be efficient in vivo with a low duty ratio, having a high duty ratio allows enzymes such as kinesin-1 to function as isolated single molecules in vivo (Howard, 1997).

The nonhydrolyzable ATP analogue AMP-PNP stabilizes a tightly bound kinesin–microtubule complex. This tight binding was exploited in the initial purifications of kinesin from tissue (Brady, 1985; Scholey et al., 1985; Vale et al., 1985). Since then, AMP-PNP has proven to be a useful tool in transient-state and steady-state kinetics experiments to elucidate kinesin mechanochemical function, in optical trapping experiments to study kinesin mechanics, and in analyses of the structure of the kinesin–microtubule complex by electron microscopy (Schnapp et al., 1990; Hirose et al., 1995; Crevel et al., 1996; Ma and Taylor, 1997a; Arnal and Wade, 1998; Gilbert et al., 1998; Rice et al., 1999; Hoenger et al., 2000; Kawaguchi and Ishiwata, 2001; Uemura et al., 2002; Asenjo et al., 2003; Rosenfeld et al., 2003; Asenjo et al., 2006). Given its widespread use, the manner by which kinesin steady-state ATPase and motility are inhibited by AMP-PNP is surprisingly poorly characterized. The mode of inhibition is variously reported to be competitive (Kuznetsov and Gelfand, 1986) or to deviate from purely competitive (Cohn et al., 1989).

A synthesis of recent work (for reviews see Asbury, 2005; Yildiz and Selvin, 2005) with the results of earlier studies (for review see Schief and Howard, 2001) strongly supports the hypothesis that uninhibited, wild-type kinesin moves by an "asymmetric hand-over-hand" mechanism in which ATP is alternately hydrolyzed by the two active sites of the enzyme. In this mechanism, the enzyme never exists in a state in which both active sites are vacant. Instead, each catalytic cycle is initiated by binding of ATP to a vacant site while the other is still

Correspondence to Jeff Gelles: gelles@brandeis.edu

The online version of this article contains supplemental material.

Abbreviation used in this paper: AMP-PNP, adenosine 5'-(β,γ-imido)triphosphate.

J. Gen. Physiol. © The Rockefeller University Press $30.00
Volume 130 Number 5 November 2007 445–455
http://www.jgp.org/cgi/doi/10.1085/jgp.200709866

occupied by an ADP molecule from the preceding cycle. Consequently, the simplest hypothesis is that AMP-PNP inhibits kinesin by a simple substrate-antagonistic mechanism, in which it acts only by binding to the single vacant site at the point in the catalytic cycle where the enzyme is waiting to bind ATP. This mechanism demands that all movement observed in mixtures of ATP and AMP-PNP is by kinesin molecules with no bound inhibitor and that binding of only a single inhibitor molecule inhibits movement.

Here, we investigated the pathways of AMP-PNP inhibition of steady-state kinesin movement by observing the nanometer-scale motion of single kinesin molecules in mixtures of ATP with varying concentrations of AMP-PNP. Microtubule-complexed single kinesin molecules in this nucleotide mixture stochastically switch between nonmoving ("pauses") and moving states ("runs") (Vugmeyster et al., 1998). We here present evidence that the moving state is a composite of two different kinds of multistep runs. Analysis of single-molecule run and pause kinetics suggests that in one of these kinds of runs, kinesin can execute continuous, processive, high-duty-ratio movement along the microtubule despite the fact that the turnover of one head is continuously blocked by bound AMP-PNP.

MATERIALS AND METHODS

Protein Expression and Purification

K401-BIO-H6 is a dimeric kinesin construct containing the first 401 residues of *Drosophila* kinesin heavy chain fused to an 87-residue region of *Escherichia coli* biotin carboxyl carrier protein (identical to K401-BIO; see Berliner et al., 1995) followed by a six-histidine tag to facilitate purification. K401-BIO-H6 was expressed from strain BL21(DE3) pLysS pWC2 and a clarified cell lysate was prepared as previously described (Berliner et al., 1995). Batch purification was initiated by mixing the lysate with Ni-NTA resin (QIAGEN) for 2 h. The mixture was poured into a column, washed with 20 mM imidazole, pH 7.2, 4 mM $MgCl_2$, 10 mM β-mercaptoethanol, 50 μM ATP and eluted with the same buffer containing 500 mM imidazole. Peak protein fractions were further purified on a MonoQ anion exchange column (GE Healthcare) with a 0–1 M NaCl gradient in 50 mM imidazole, pH 6.7, 4 mM $MgCl_2$, 10 mM β-mercaptoethanol, 50 μM ATP over 25 ml in 33 min. Peak ATPase fractions were identified using the assay described in the online supplemental materials, pooled, supplemented with 1 M sucrose, frozen in liquid nitrogen, and stored at −80°C.

Motility Assay

Motility assays were done as described previously (Berliner et al., 1995), except that 150-nm diameter beads were used. Enzyme and beads were mixed in a mole ratio such that <3% of the beads have two active enzyme molecules bound. Imaging and nanometer-scale bead position measurements (33-ms time interval) were performed as previously described (Vugmeyster et al., 1998) to yield time records of the bead position projected onto the microtubule axis. The bead position measurements made here have spatial precision that is improved over that obtained previously (Vugmeyster et al., 1998); this was achieved using larger beads that yield higher image contrast, optimizing the camera magnification for best precision, reducing the concentration of beads to minimize noise from the diffusion of beads free in solution, and digitizing video directly from the camera, rather than from videotape, in order to reduce electronic noise in the images. The improved precision, together with larger datasets, longer records, and/or wider ranges of AMP-PNP concentrations than in earlier studies (Vugmeyster et al., 1998; Guydosh and Block, 2006), made the existence of the two separate classes of runs more clearly evident in these experiments than in previous work.

Run/Pause Event Detection

Each point in the bead position records was classified as belonging to a run or pause using an objective discrimination algorithm. Intervals in which the instantaneous velocity was ≥+180 nm s^{-1} were provisionally classified as runs (by convention, movement in the direction of net movement for each record was defined as positive). An isolated single point below this velocity threshold was scored as being above the threshold for the purpose of this classification (Colquhoun and Sigworth, 1995). The pause/run discrimination was iteratively refined by reclassifying as part of the flanking pauses any run that resulted in a net displacement (calculated as the difference between the means of the pairs of points immediately preceding and following the run) of <+6 nm. To avoid counting events terminated by bead dissociation or irreversible binding, the events (runs or pauses) that began and ended each record were excluded from further analysis, as was the last run of each record. Events shorter than a threshold value (t_{min}) of pause duration 0.066 s or run length 12 nm could not be efficiently detected and therefore were also excluded. In experimental records (for example, those in 0.5 mM ATP plus 0.5 mM AMP-PNP) this discrimination algorithm detected 80 pauses of duration ≥0.066 s for every 10,000 nm of movement and 322 runs of length ≥6 nm for every 1,000 s of record. In contrast, the numbers of runs detected in controls with 0.5 mM AMP-PNP and no ATP was negligible (3.3 per 1,000 s), as was the number of pauses in controls with 0.5 mM ATP and no AMP-PNP (1.66 per 10,000 nm).

Analysis of Event Distributions

Run length and pause lifetime distributions were compiled in histograms with variable bin widths and plotted as probability densities computed by scaling the number of events in each bin $n(t)$ centered at time t by bin width $w(t)$ and normalizing by the total number of events in the histogram (N). Pause lifetime distributions were fit (Levenberg-Marquardt algorithm) to the triexponential ($j = 3$) probability density function

$$\frac{n(t)}{Nw(t)} = \sum_{i=1}^{j} \frac{n_i}{N\tau_i} \exp(-t/\tau_i) \Big/ \sum_{i=1}^{j} \frac{n_i}{N} \exp(-t_{\min}/\tau_i),$$

where τ_i and n_i are adjusted to determine the time constants and corresponding numbers of events, respectively, except that

$$n_j = N - \sum_{i=1}^{j-1} n_i$$

(Colquhoun and Sigworth, 1995). The run length distribution was fit to the same equation except that the distribution was biexponential ($j = 2$) and the independent variable was length instead of time. All fits were weighted by the reciprocal of the variance $\sigma^2 = n(t) / (N\, w(t))^2$. Fractional amplitudes of the exponential terms were calculated as $a_i = n_i / N$. The standard error (SE) of a_3 was computed as $(\sigma_{11}^2 + \sigma_{22}^2 + 2\sigma_{12}^2)^{0.5}$, where σ_{11} and σ_{22} are standard errors of a_1 and a_2 determined from the triexponential fits and σ_{12}^2 is the covariance. Distributions were further corrected for under/overcounted events and then refit (see online supplemental material, available at http://www.jgp.org/cgi/content/full/jgp.200709866/DC1). The exponential function is an approximation to the true short run length distribution, which is

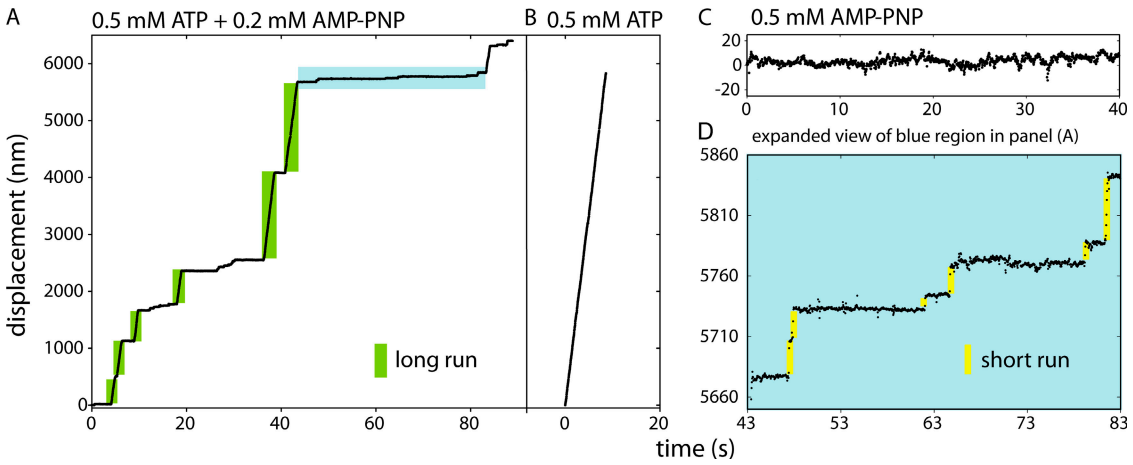

Figure 1. Movement on microtubules of single kinesin molecules tagged with streptavidin-coated beads. Graphs show bead position along the microtubule axis as a function of time in 0.5 mM ATP plus 0.2 mM AMP-PNP (A and D), 0.5 mM ATP only (B), or 0.5 mM AMP-PNP only (C). D is an expanded view of the blue region in A. Green and yellow regions in A and D mark examples of long and short runs, respectively. Note expanded scales in C and D.

expected to be geometric (see Appendix). Refitting the short run distribution with the exact function revealed that the approximation leads to only a small underestimation of the mean short run lengths (for example, 17.8 vs. 13.3 nm mean short run length at 0.5 mM ATP and 0.2 mM AMP-PNP).

Online Supplemental Material

The online supplemental material for this paper (available at http://www.jgp.org/cgi/content/full/jgp.200709866/DC1) contains (a) supplementary data describing kinesin motility at subsaturating ATP/AMP-PNP concentrations (Fig. S1), discussion on population heterogeneity, simulation of one-step and one- or two-step short run models (Figs. S2 and S3), short-run duty ratio calculation, AMP-PNP inhibition of kinesin steady-state ATPase (Fig. S4), correlation analysis, and sampling bias at low and high AMP-PNP; as well as (b) supplementary methods describing the ATPase assay, correction of run- and pause-length distributions, and estimation of the rate constants shown in Fig. 5 (A and B).

RESULTS

Movement of Single Kinesin Molecules in Mixtures of ATP and AMP-PNP

In the presence of ATP and AMP-PNP, beads driven by single kinesin molecules alternate between intervals of continuous ATP-driven movement (runs) and AMP-PNP-induced halts (pauses) (Vugmeyster et al., 1998; Guydosh and Block, 2006). To further characterize the nature of the inhibition and the effect of AMP-PNP on kinesin motility, we examined with improved precision single-molecule movements in mixtures of ATP (at a fixed 0.5 mM concentration) and AMP-PNP at a wide range of concentrations. An example data record displaying runs and pauses is shown (Fig. 1 A).

In control experiments (0.5 mM ATP in the absence of AMP-PNP), enzyme movement is continuous with essentially no pausing (Fig. 1 B). Individual 8-nm steps were not resolved: at this high movement velocity, 747 ± 88 (SD) nm/s, there were on average approximately three steps between each pair of successive time points (33 ms) in the movement record. Conversely, in 0.5 mM AMP-PNP in the absence of ATP, no significant unidirectional movement was observed for the duration of the experiment (Fig. 1 C).

When both ATP and AMP-PNP are present, the enzyme alternates between runs and pauses (Fig. 1 A). In some single runs the enzyme traverses long distances corresponding to hundreds of 8-nm steps. In addition to these "long runs," the records also contain a large number of short-distance, unidirectional movements (Fig. 1 D). In these "short runs," the enzyme moves a distance corresponding to only a few sequential 8-nm steps before it enters a pause. The mean velocity during the longest (>500 nm) observed runs (674 ± 83 nm/s) is similar to that in the absence of AMP-PNP (747 ± 88 nm/s), consistent with the hypothesis (Vugmeyster et al., 1998) that these runs arise from uninhibited turnover of the enzyme. The short run velocity could not be accurately determined because of the limited time resolution and the small distances moved in these events. However, short runs were at least 8 nm in length and their duration was often no longer than the 33-ms time resolution of the recordings. This suggests that the velocity during these runs is >8 nm/0.033 s = 240 nm/s.

AMP-PNP Concentration Dependence of Long and Short Run Lengths

The observation of numerous runs hundreds of steps long in the same dataset that contains many runs two orders of magnitude shorter raises the possibility that there exist two or more distinct classes of runs. To test this hypothesis, we measured the distribution of run lengths at various nucleotide concentrations. Under all conditions tested (0.5 mM ATP plus 0.05–3 mM AMP-PNP), the distributions are biphasic (e.g., Fig. 2 A).

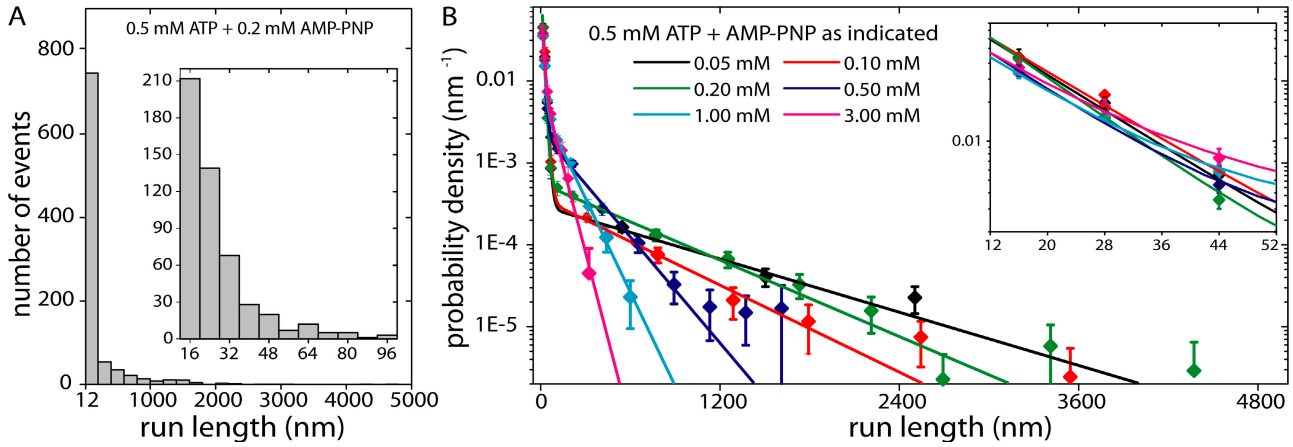

Figure 2. Distribution of run lengths for single kinesin molecules in mixtures of ATP and AMP-PNP. (A) Histogram of all run lengths larger than 12 nm in 0.5 mM ATP and 0.2 mM AMP-PNP. Inset: expanded histogram of the subset of run lengths between 12 and 100 nm. (B) Histograms of run lengths in 0.5 mM ATP plus various concentrations of AMP-PNP (note logarithmic scale). Numbers of observed runs at different AMP-PNP concentrations: 0.05 mM, 336; 0.1 mM, 603; 0.2 mM, 712; 0.5 mM, 731; 1 mM, 597; 3 mM, 255. Solid lines are bi-exponential probability density functions fit to the data. Inset shows expanded view of the same data and fits. Error bars are the standard deviations σ_{corr} (see online supplemental material).

We observe long runs with a range of lengths, together with a high number of multiple-step short runs (Fig. 2 A). The distributions are clearly inconsistent with a mono-exponential probability density function ($P < 0.0005$ in the 0.05–1 mM AMP-PNP concentration range and $P = 0.02$ at 3 mM AMP-PNP) but fit to a bi-exponential function (Fig. 2 B), confirming that there are at least two classes of runs in these nucleotide mixtures (Colquhoun and Sigworth, 1995). The two exponential components have mean lengths (e.g., 12 ± 1 and 801 ± 111 nm in 0.5 mM ATP plus 0.05 mM AMP-PNP) that under some conditions differ by >60-fold. Thus, during the long run class enzyme molecules are more than an order of magnitude less susceptible to AMP-PNP–induced pausing than they are during the short run class. Bi-exponential run length distributions were also obtained at subsaturating nucleotide concentrations (see online supplemental material, available at http://www.jgp.org/cgi/content/full/jgp.200709866/DC1). This data suggests that the existence of two types of runs depends on the ratio of ATP to AMP-PNP, not on their absolute concentrations.

Do the two classes of runs originate from distinct populations of enzyme molecules with differing properties, or can an individual kinesin molecule perform both kinds of runs in the course of a single association with a microtubule? Examination of single-molecule records shows the latter; individual records (e.g., Fig. 1 A) often contain both very long and very short runs (see online supplemental material). Long individual records usually produce bi-exponential run length distributions resembling that of the dataset as a whole, further supporting the notion that the same individual kinesin molecule is capable of both classes of runs. In addition, the fact that both classes of runs are frequently seen in single bead records excludes the possibility that the short runs come only from a small subpopulation of beads moved by more than one kinesin molecule, since independent experiments demonstrate that the fraction of beads in that subpopulation is vanishingly small (see Materials and methods).

To help determine the cause of the differing properties of long and short runs, we examined the dependence of their mean run lengths on AMP-PNP concentration. Since pauses are detected only in the presence of AMP-PNP, the simplest hypothesis is that a pause begins when a molecule of AMP-PNP binds to a kinesin molecule that has been moving processively along a microtubule. In this scenario, the rate of pause entry is expected to increase (and the mean run length is thus expected to decrease) with increasing AMP-PNP concentrations. Consistent with this expectation, the mean length of the long runs, obtained from fitting the run length distributions (Fig. 2 B), decreases from 558 ± 39 nm to 62 ± 7 nm as AMP-PNP is increased from 0.2 to 3.0 mM in the presence of constant 0.5 mM ATP. The observed first order "rate constants" for exiting the long run (i.e., the reciprocals of the mean run lengths) are roughly proportional to AMP-PNP concentration (Fig. 3 A); the small deviations from proportionality apparent at low (50–100 μM) and high (3.0 mM) AMP-PNP concentrations may arise from sampling bias (see online supplemental material). In summary, the data are consistent with the idea that long runs terminate by an AMP-PNP binding event, precisely the behavior expected from a simple inhibition mechanism.

Since no significant pausing of any sort is seen in the absence of AMP-PNP, it is likely that all paused kinesin molecules have AMP-PNP bound. Surprisingly, the mean run length of the short run is essentially independent

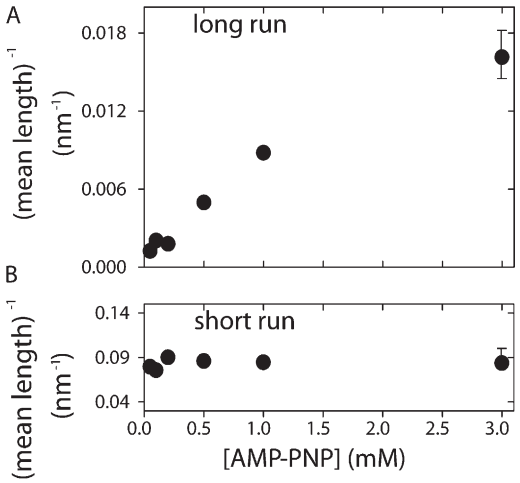

Figure 3. Rate constants for exiting long (A) and short (B) runs in 0.5 mM ATP plus the indicated concentration of AMP-PNP. Rate constants are computed as the reciprocals of the long and short mean run lengths determined from the fits of the distributions in Fig. 2. Standard errors are shown when the error bars are larger than the plotting symbol. The relative amplitude of the short run component of the bi-exponential fit ranged from 0.9 at 0.1 mM AMP-PNP to 0.7 at 3.0 mM AMP-PNP. The reciprocal of the mean length of the long or short runs corresponds to the probability of exiting the run per unit distance moved. Even though this quantity has dimensions of inverse distance and is thus more precisely a "length constant"; we colloquially refer to it as a "rate constant" in this paper.

of AMP-PNP concentration in the tested range (Fig. 3 B). The AMP-PNP–independent run length is unexpected because it implies that transition from a short run to a pause is not triggered by AMP-PNP binding. This observation, together with the observation that neither short runs nor pauses are observed in the absence of AMP-PNP, strongly suggests that the enzyme has AMP-PNP bound throughout the duration of the short run. Continuous occupancy of one active site by AMP-PNP during the multiple catalytic cycles of a short run is the only straightforward explanation for why enzyme in a short run enters the paused state at the end of the run (no pausing is seen the absence of inhibitor), but that the rate of entering the pause is independent of the AMP-PNP:ATP concentration ratio over a wide range. In this scenario, pausing after a short run is caused by a conformational isomerization of a kinesin–microtubule complex that already had a bound molecule of AMP-PNP but nevertheless continued to move.

Short Runs Are Sequences of Multiple Steps

The short runs are short; their mean length (~12 nm; Fig. 3) is equivalent to between one and two 8-nm steps. Nevertheless, short runs of lengths corresponding to three or more consecutive 8-nm steps were frequently observed (Fig. 2 A, inset). Furthermore, the observation that the short runs are exponentially distributed in length (Fig. 2) strongly suggests that these events are true runs that in general consist of a sequence of steps, not merely isolated single 8-nm movements. Numerical simulations (see online supplementary material) confirm that the observed run length distributions are inconsistent with a mechanism in which the enzyme moves in a combination of long runs and randomly distributed isolated 8-nm steps. A mechanism in which the enzyme can take two steps at most during the short run is also inconsistent with the observed distribution (see online supplemental material). Thus, the observed distribution of short run lengths suggest that these events are true runs that consist of stochastic sequences of multiple 8-nm steps. Because the short runs in general consist of multiple 8-nm steps, they are distinct from the backward and forward single-step movements reported previously for kinesin molecules under load (Coppin et al., 1996; Nishiyama et al., 2002; Guydosh and Block, 2006).

Evidence for Multiple AMP-PNP–Inhibited States of Kinesin

The kinesin active site has different chemical properties depending on whether the head is in the leading or trailing position on the microtubule (Hackney, 1994; Rosenfeld et al., 2003; Guydosh and Block, 2006). Thus, it is possible in principle that there are three (or more) distinct inhibited states of the enzyme: AMP-PNP may be bound to the leading head, the trailing head, or both. To test for the presence of such multiple states, we compiled lifetime distributions for the pauses observed in our experiments (Fig. 4 A, symbols). The pause lifetime distribution was clearly at least bi-exponential (with mean lifetimes ~0.2 and ~1.5 s) at low inhibitor concentrations, consistent with the presence of two or more paused species. At higher AMP-PNP concentrations (1–3 mM), additional very long pauses (mean lifetime ~9 s) were observed and the distribution of pause lifetimes was clearly at least tri-exponential (e.g., P = 0.03 at 3 mM AMP-PNP). When distributions from all AMP-PNP concentrations were independently fit to a tri-exponential function, little or no dependence of the three mean pause lifetimes on AMP-PNP concentration was observed (Fig. 4 B, symbols). This is the result predicted by simple models in which inhibition is terminated either by a conformational change or by dissociation of AMP-PNP. There was no systematic variation with inhibitor concentration in the relative amplitudes of the first and second exponential components, but the prevalence of the longest pauses increased with increasing AMP-PNP concentrations (Fig. 4 C; green triangles). This observation is consistent with certain mechanisms in which the longest pauses are from an enzyme species with two bound AMP-PNP molecules while the shorter pauses have only a single bound inhibitor, but other interpretations are also possible.

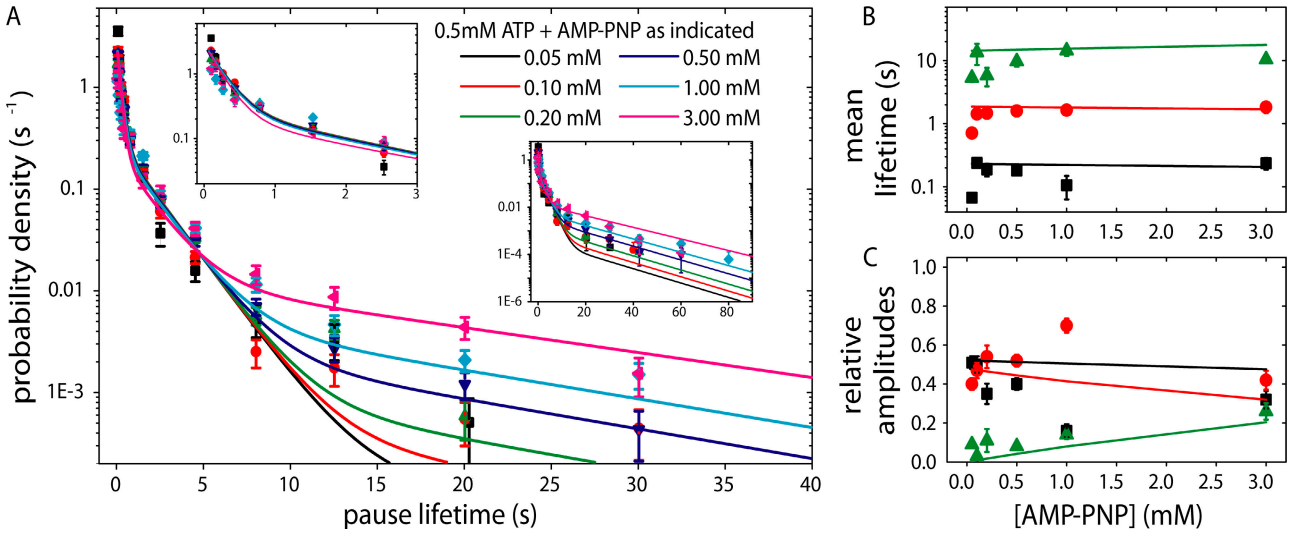

Figure 4. (A) Pause lifetimes. Histograms of pause lifetimes observed (symbols) at the indicated nucleotide concentrations. Numbers of observed pauses at different AMP-PNP concentrations: 0.05 mM, 416; 0.1 mM, 770; 0.2 mM, 947; 0.5 mM, 900; 1 mM, 737; 3 mM, 347. Lines are the predicted tri-exponential probability density functions for the proposed mechanism and rate constants (Fig. 5 B; see Discussion). Insets show expanded views of the same data. Mean lifetimes (B) and fractional amplitudes (C) of the long (green), medium (red), and short (black) terms in the tri-exponential probability density function. SE of the exponential terms were obtained from unconstrained fits (see Materials and methods). Lines in B and C are the parameters predicted by the proposed mechanism.

Short Runs are Processive, High-Duty-Ratio Movements

During short runs, we do not observe any back-and-forth fluctuation of the position of the enzyme on the microtubule lattice. This is the hallmark of a high-duty-ratio mechanism, in which the enzyme spends all or nearly all of its catalytic cycle tightly bound to the microtubule in state(s) that do not allow diffusional sliding in the direction of the microtubule axis (Young et al., 1998; Inoue et al., 2001). To estimate the duty ratio of the short runs, the total number of isolated single-step 8-nm displacements made by the enzyme toward the plus and minus ends were separately counted. The ratio of the number of displacements in the plus direction to the total number of single-step displacements indicates that most observed motions corresponding in size to an isolated 8-nm step are toward the plus end (~80%). Assuming a simple model where all backward displacements and an equal number of forward displacements are due to free diffusive sliding of a weakly or unbound intermediate leads to an estimated short-run duty ratio of >0.99 (see online supplemental material). Thus, like the long runs and the movement of kinesin in the absence of AMP-PNP, the short runs have a duty ratio close to unity.

DISCUSSION

Our single-molecule experiments show that the motility of kinesin in mixtures of ATP and AMP-PNP is more complex than expected if AMP-PNP acts by a simple substrate-antagonistic mechanism. In such a mechanism, there is a single intermediate in which one enzyme active site is unoccupied (the "waiting for ATP" state) and the substrate and inhibitor compete for and can bind to only this state. This type of mechanism predicts that the enzyme should move in a single type of run, the mean length of which is inversely proportional to AMP-PNP concentration. Inconsistent with this prediction, we detect two classes of runs. In both classes, kinesin often moves distances corresponding to multiple 8-nm steps. Both classes of movement are largely or completely unidirectional and thus are ATP driven. The mean distance moved during the long runs is inversely proportional to AMP-PNP concentration as expected for the simple substrate-antagonistic mechanism; in contrast, the distance moved during the short runs is independent of AMP-PNP concentration.

The data reveal similarly complex behavior in the pauses that terminate runs of enzyme movement. We observe multiple pause lifetimes, revealing the presence of at least three distinct AMP-PNP–inhibited states of microtubule-bound kinesin.

Earlier work with essentially the same single-molecule motility assay used here did not characterize the run length distribution and reported only one exponential component in the distribution of AMP-PNP–induced pause lifetimes (Vugmeyster et al., 1998). Additional pause lifetime components were resolved in the present study because of an improved ability to detect short pauses (minimum detected pause duration 0.06 vs. 0.23 s), the analysis of behavior at higher AMP-PNP concentrations (3.0 vs. 0.5 mM), and the collection of larger datasets that enabled reliable detection of the rarer, long-lived pauses.

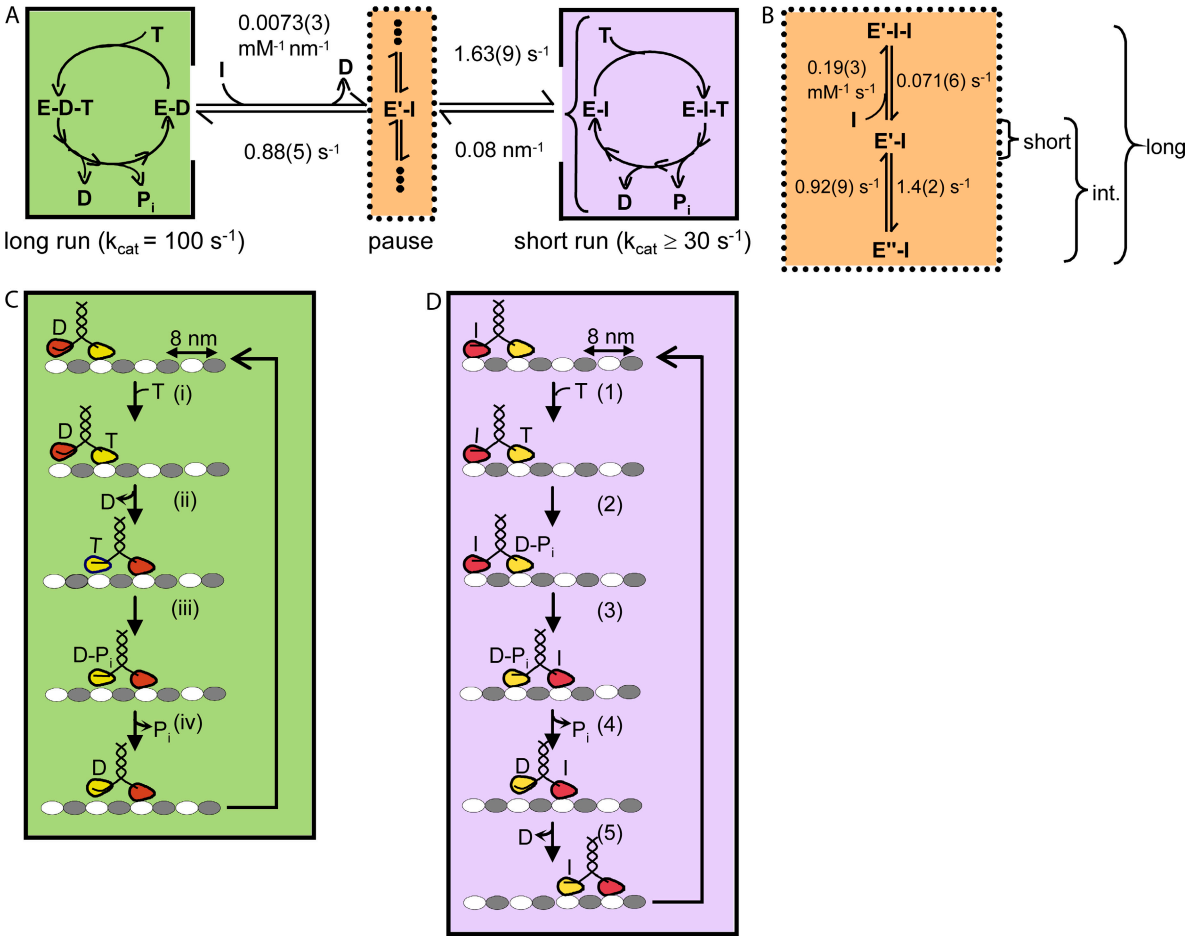

Figure 5. A two-cycle kinetic scheme consistent with the observed characteristics of kinesin inhibition by AMP-PNP. E, microtubule-bound dimeric kinesin; T, ATP; D, ADP; I, AMP-PNP; P_i, inorganic phosphate. (A) Run-state catalytic cycles and rate constants for conversion between run and pause states. Green and violet boxes each contain a complete catalytic cycle; these correspond to the long and short runs, respectively. Not all cycle intermediates are explicitly shown. In the short-run cycle all intermediates contain a single bound AMP-PNP. The AMP-PNP binding that terminates the long run is assumed to trigger ADP release from the tethered head (Ma and Taylor, 1997a; Gilbert et al., 1998). The bracket indicates that the species that isomerizes to terminate the short run by producing the inhibited conformation E'-I is not known. Mechanisms in which any individual or combination of catalytic cycle intermediates isomerize are consistent with the data. Numbers in parentheses are the SE of the least significant digit of the rate constant. (B) One possible arrangement of inhibited species and the rate constants consistent with the observed tri-exponential pause lifetime distribution. The set of species populated in each type of pause is indicated (brackets). E'-I and E"-I represent two different inhibited species, each with a single AMP-PNP bound, and E'-I-I represents an inhibited species with two bound AMP-PNP. (C and D) Detailed movement mechanisms postulated for the long-run cycle (C; identical to a widely accepted mechanism for kinesin movement in the absence of inhibitor: Rosenfeld et al., 2003; Guydosh and Block, 2006) and the short-run cycle (D; a speculative proposal based on hand-over-hand movement). In both columns, kinesin is shown stepping toward the plus end (at right) of a microtubule protofilament composed of alternating α-tubulin (gray oval) and β-tubulin (white oval) subunits. The two kinesin heads are colored red and yellow for identification. In the trailing head, the neck linker is shown as docked (straight line) or undocked (curved line). In both mechanisms, the cycle begins with ATP binding to the empty lead head (C, step i, and D, step 1). In the conventional mechanism, rapid forward movement of the trailing head (C, step ii) is facilitated by the presence of ADP in the trailing head active site, which allows rapid head dissociation from the microtubule (Ma and Taylor, 1997b; Uemura et al., 2002). The analogous step in the one-site mechanism (D, step 3) involves forward movement of the AMP-PNP–bound head. The cycle is completed by a second 8-nm step accompanied by ADP release (D, step 5) that is analogous to that in the conventional mechanism (C, step ii) but has AMP-PNP instead of ATP in the leading head. In both cases, the post-step configuration is stabilized by ADP release. Some studies (Rosenfeld et al., 2003; Auerbach and Johnson, 2005; Guydosh and Block, 2006) suggest that binding of ATP to the state produced by step ii in C is extremely slow, presumably due to neck linker strain, but the binding rate has only been inferred from indirect measurements, not measured directly. In the proposed single-site catalysis mechanism, ATP binding to the analogous state (D, step 1) must be at least as fast as the short run k_{cat}.

More recently, Guydosh and Block (2006) used optical trapping to analyze movement of kinesin under opposing mechanical force in mixtures of ATP and the inhibitor BeF_x or AMP-PNP. These investigators also observed run/pause behavior as reported here and in our earlier study (Vugmeyster et al., 1998). They did not note a bi-exponential run length distribution, possibly because the forces from the optical trap either suppress

short runs or reduce the total distance moved by individual molecules, which in turn would make the distinction between long and short runs less apparent. We do not see the brief back-and-forth stepping seen in the optical trap, possibly because our experiments are conducted at zero applied force.

What do the two-component run-length distributions tell us about the mechanism of kinesin movement? Since both ATP and AMP-PNP are present at concentrations of similar magnitude in some of the experiments, the existence of continuous long runs ~100 or more steps in length implies that these events arise from a catalytic cycle that is highly resistant to AMP-PNP inhibition. In kinesin-1, ATP binding triggers the release of ADP from the other head, allowing the enzyme to take an 8-nm forward step. AMP-PNP also triggers ADP release and we assume this AMP-PNP–triggered ADP release is necessary for the enzyme to switch from a long run into a pause (Fig. 5 A). Therefore, it is not surprising that kinesin can make runs of hundreds of steps at millimolar concentrations of both ATP and AMP-PNP, since it is already known that ATP-stimulated ADP release is 12- to 50-fold faster than AMP-PNP–stimulated ADP release at these concentrations (Ma and Taylor, 1997a; Gilbert et al., 1998). The substantial difference in kinetics seen with these two very similar compounds might result from subtle structural differences that cause the ADP–kinesin–AMP-PNP complex to have a higher rate of AMP-PNP dissociation than the rate of ATP dissociation from ADP–kinesin–ATP.

Unlike those in long runs, kinesin molecules in short runs are much more prone to pausing; they usually pass into a kinetically stable paused state after taking only a few consecutive steps. A simple two-cycle kinetic scheme consistent with the observed run-length distributions of individual kinesin molecules in ATP/AMP-PNP mixtures is illustrated in Fig. 5 A. In this mechanism, the long run has a catalytic cycle identical to that of the uninhibited enzyme. The short run cycle consists of an entirely different set of intermediates, all of which have AMP-PNP bound to one of the two heads. The two kinds of runs terminate by different processes: the long run by AMP-PNP binding and the short run by an AMP-PNP–independent conformational isomerization step. In such a mechanism, (a) the velocity of long runs will equal that in the absence of AMP-PNP, (b) the apparent first-order rate constant for exiting the long run will be proportional to AMP-PNP concentration, and (c) the short run exit rate constant will be independent of AMP-PNP concentration. These are precisely the behaviors observed (Figs. 1 and 3). The mechanism predicts that ATPase kinetics should deviate from those of a simple substrate-antagonistic mechanism; such deviations are in fact observed (see online supplemental material).

The novel feature of the proposed mechanism, that there are two distinct cycles that have no intermediates in common, is dictated by the bi-exponential run length distribution (see Appendix). A mechanism in which the two cycles have one or more common intermediates that are traversed in every cycle will produce only a mono-exponential run length distribution. An alternative explanation for the bi-exponential run length distribution is that the enzyme has only one catalytic cycle (the widely accepted alternating sites mechanism) and that activity is allosterically modulated by slow binding and release of AMP-PNP to site(s) other than the two active sites of dimeric kinesin. However, we view such a mechanism as unlikely because both the structure and nucleotide binding properties of the enzyme have been extensively studied and there is no evidence for nucleotide binding outside of the active sites.

The observed tri-exponential distributions of pause lifetimes, together with the observation that no pausing is detected in the absence of AMP-PNP, imply the presence of at least three AMP-PNP–inhibited kinesin species. In an attempt to determine which of the two catalytic cycles the paused species originate from, we tested whether runs of a particular length tended to be followed by characteristically long or short pauses. We also examined whether long and short runs were distributed randomly or whether they tended to occur in clusters. No significant correlations of these types were detected (see online supplemental data). Taken together, these results are consistent with a simple mechanism in which enzyme molecules exiting from or entering into either type of run do so through a single, common inhibited species (E'-I in Fig. 5 A). We emphasize that the data do not unambiguously define the arrangements of the three (or more) paused species within the dotted rectangle in Fig. 5 A. One example arrangement with rate constants that produce pause distributions consistent with the data (Fig. 4, B and C) is shown in Fig. 5 B. However, alternative arrangements of the three pause states (not depicted) also can produce lifetime distributions that agree with the data within experimental uncertainty.

The results reported here suggest that kinesin is capable of processive high-duty-ratio movement in short runs driven by an unconventional mechanism in which only one head is catalytically active. Certain one-headed kinesin family members like Kif1A monomers (Okada et al., 1995) and even an artificial one-headed fusion of kinesin-1 with biotin-dependent transcarboxylase (Inoue et al., 2001) show processive movement. However, these molecules do not generate movement with a duty ratio near unity. Instead, such molecules spend significant parts of each catalytic cycles in states that allow diffusional sliding of the enzyme along the microtubule axis. The novel feature of our results is that we detect multi-step runs (albeit short ones) of high-duty-ratio movement that are driven by turnover of only one active site, contradicting the common conception that alternating-sites hydrolysis is required for high-duty-ratio movement.

The experimental results imply the existence of two independent catalytic cycles. The long runs appear identical to the movement of kinesin in the absence of inhibitor. We therefore propose that the detailed mechanism of the long run catalytic cycle is identical to that of kinesin in the absence of inhibitor (Fig. 5 C). In contrast, the short runs must occur through a novel, single-site catalysis mechanism, the details of which are not fully established by the experimental results. One possibility is that single-site catalysis drives movement through a hand-over-hand process (as in the absence of inhibitor), but that only one ATP is hydrolyzed for every two 8-nm steps. (Since neither odd nor even numbers of 8-nm steps predominate in the short run length distributions [Fig. 2, insets], a mechanism with alternating, nonidentical 8-nm steps is consistent with the observations only if there are two or more entry or exit pathways from the short run; these multiple pathways are shown as a single lumped step in Fig. 5 A.) ATP hydrolysis in only every other step would require that the mechanisms of the even- and odd-numbered steps are different; one possible scenario for this is shown in the right column of Fig. 5 D. In this hypothesis, the first 8-nm step (Fig. 5 D, step 3) requires detachment and forward movement of an AMP-PNP–bound head. This step is expected to be slower than the 8-nm step of the long run (Fig. 5 C, step ii) as AMP-PNP induces a more kinetically stable head–microtubule interaction than does ADP (Hancock and Howard, 1999). We cannot reliably predict whether this kinetic deficit would be severe enough to substantially reduce the overall rate of turnover. However, laser tweezers experiments suggest that a trailing, AMP-PNP–bound head can dissociate at a significant rate (Guydosh, N., and Block, S., personal communication). In contrast to the first 8-nm step, the second 8-nm step (Fig. 5 D, step 5) is very similar to stepping by uninhibited kinesin (Fig. 5 C, step ii). We emphasize that the Fig. 5 D mechanism is speculative; it merely illustrates one possible way that high-duty-ratio movement could be driven by turnover of a single head. Further experiments will be required to differentiate this from other possible mechanisms for short-run movement.

The short-run mechanism proposed in Fig. 5 D bears a superficial resemblance to mechanisms proposed to explain kinetic "limping" in kinesin-1 homodimers and wild-type/mutant heterodimers (Hoenger et al., 2000; Kaseda et al., 2002; Asbury et al., 2003; Kaseda et al., 2003). Our proposal has in common with these mechanisms the idea that odd- and even-numbered 8-nm steps occur through structurally distinct reaction pathways; these alternate steps may therefore occur with different characteristic rates. However, there is a critical difference: the proposed limping mechanisms all involve alternating ATP hydrolysis by the two heads. In contrast, the short run mechanism is a one-site mechanism in which only one head hydrolyzes ATP and the other active site is continuously occupied by AMP-PNP. Thus the mechanism proposed in Fig. 5 D is fundamentally different from those hypothesized to explain kinesin limping. Despite the fact that its catalysis is blocked, microtubule binding of the inhibited head in the short-run mechanism functions to help maintain the association of the dimer with the microtubule. In this sense, the function of the inhibited head is analogous to that proposed for the Vik1 inactive head in the Kar3/Vik1 kinesin-14 heterodimer (Allingham et al., 2007).

In summary, in mixtures of ATP and AMP-PNP, we see a new mode of high-duty-ratio processive kinesin movement in which only one of the two active sites of the enzyme is available for ATP hydrolysis. The existence of two kinesin mechanochemical cycles with entirely different intermediates is intriguing, although there are precedents for alternative catalytic pathways in other multisubunit enzymes (Boyer, 2002). Our studies on kinesin strongly suggest that different mechanochemical cycles exist in the simultaneous presence of substrate and inhibitor. It remains to be seen whether there are multiple modes of ATP-driven kinesin movement in the presence of substrate alone.

APPENDIX

Run Length Distribution for Catalytic Cycles with Common Intermediates

In this paper we observe that the distribution of run lengths for kinesin-1 movement in mixtures of ATP and AMP-PNP is bi-exponential. Based on this observation, we conclude that (a) the kinesin mechanism under these conditions consists of two (or more) different mechanochemical cycles, and that (b) two cycles cannot produce the observed behavior if the cycles share any common catalytic intermediates. In this Appendix, we briefly describe the reasoning underlying these two conclusions.

Kinesin-1 and similar high-duty-ratio processive motor enzymes catalyze a highly energetically favorable chemical process, the hydrolysis of ATP. Consequently, a motor enzyme catalytic cycle contains one or more steps that are essentially irreversible under physiological conditions. Each cycle of such a motor is typically accompanied by a fixed-size step movement of the motor along its track.

Consider a highly simplified motor mechanism in which one of the intermediate states in the cycle can react to form an inhibited species:

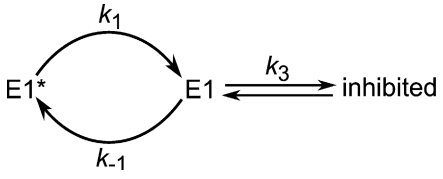

(SCHEME 1)

(For this and other mechanisms shown in this Appendix, the cycle is shown as a simple two-step loop. Binding of substrate, release of hydrolysis products, and stepping of the enzyme along the track occur during the cycle but are not shown explicitly.) In this mechanism, there is a fixed probability per cycle $\lambda = k_3/(k_3 + k_{-1})$ of entering the inhibited state. This probability is independent of the rate of the reaction by which the molecule leaves the inhibited state to resume a run (Scheme 1, reverse arrow).

If $\lambda << 1$, the enzyme will make runs of multiple cycles (and therefore multiple steps) before it is inhibited, and the probability of the run terminating after precisely n steps follows the geometric distribution $P(n) = \lambda(1 - \lambda)^n$. Casting this expression in terms of the distance moved $x = nd$, where d is the distance moved by the enzyme in one catalytic cycle, we obtain the probability density function $p(x) = (\lambda/d)(1 - \lambda)^{x/d}$. In the limit $\lambda/2 << 1$, this is well approximated by the exponential form $p(x) \cong (\lambda/d)\exp(-\lambda x/d)$. Mechanisms with more than two steps in the cycle will also have a well-defined λ provided that they contain only a single cycle. Therefore, even for these more elaborate mechanisms the probability of terminating a run will be described by a single-exponential function when $\lambda << 1$.

To obtain a bi-exponential run length distribution like that observed in the paper, a motor mechanism must have at least two cycles. An example is

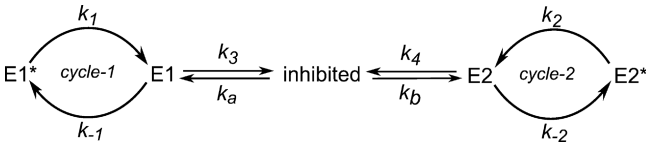

(SCHEME 2)

in which a molecule leaving the inhibited state will at random enter either cycle-1 (with entry probability $\kappa_1 = k_a/[k_a + k_b]$) or cycle-2 (with entry probability $\kappa_2 = 1 - \kappa_1 = k_b/[k_a + k_b]$). Once cycling, the probability per cycle of returning to the inhibited state is $\lambda_1 = k_3/(k_3 + k_{-1})$ for molecules in cycle-1 and $\lambda_2 = k_4/(k_4 + k_{-2})$ for molecules in cycle-2. The overall run length probability density (including runs from both cycle-1 and cycle-2) will have the bi-exponential form $p(x) \cong (\kappa_1\lambda_1/d)\exp(-\lambda_1 x/d) + (\kappa_2\lambda_2/d)\exp(-\lambda_2 x/d)$. When $\lambda_2 >> \lambda_1$, the molecule executing a run in cycle-2 will have a characteristic run length much shorter than when in cycle-1. Runs can have two different characteristic lengths because the molecule retains a fixed "memory" of which cycle it is operating in during a run; the mechanism has no pathway that allows molecules to pass from one cycle to the other during the course of a single run.

Finally, we consider the situation if cycle-1 and cycle-2 are no longer fully distinct but instead share one (or more) common intermediates. In this example,

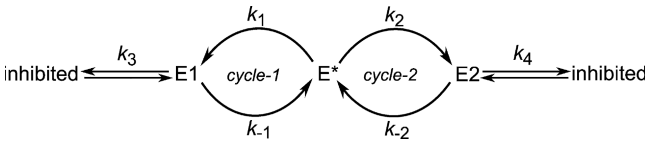

(SCHEME 3)

cycle-1 and cycle-2 share the common intermediate, E*. Each enzyme molecule passes through this intermediate in every catalytic cycle. Starting in E*, the molecule will either execute cycle-1 (with probability $k_1/[k_2 + k_1]$) or cycle-2 (with probability $k_2/[k_2 + k_1]$). In a single transit through cycle-1 or cycle-2, the enzyme has probabilities $k_3/[k_3 + k_{-1}]$ and $k_4/[k_4 + k_{-2}]$, respectively, of entering the inhibited state. Thus, the overall probability of entering the inhibited state in a single transit from E* to E* is the constant

$$\lambda = \frac{k_1}{k_2 + k_1}\left(\frac{k_3}{k_3 + k_{-1}}\right) + \frac{k_2}{k_2 + k_1}\left(\frac{k_4}{k_4 + k_{-2}}\right).$$

In essence, when cycles share a common intermediate, molecules leaving this state make a random choice, irrespective of their past history, of which cycle to enter. Every molecule thus has the same fixed probability λ of entering the inhibited state, resulting in a single-exponential run length distribution.

Even though the cycles considered here are highly simplified in that they contain only two steps and only steps that are irreversible, the conclusions reached are more general since any sequence of reaction steps that contains at least one irreversible step can at steady state be approximated by a single irreversible step with an aggregate rate constant (Fersht, 1985).

We thank Micah Hollis-Symynkywicz for his contribution to the project and Todd Thoresen, Doug Martin, Feng Wang, and Johnson Chung for extensive discussions. Thanks to Chris Miller and Larry Friedman for insightful comments on the manuscript.

This work was supported by the National Institute of General Medical Sciences.

Angus C. Nairn served as editor.

Submitted: 6 August 2007
Accepted: 5 October 2007

REFERENCES

Allingham, J.S., L.R. Sproul, I. Rayment, and S.P. Gilbert. 2007. Vik1 modulates microtubule-Kar3 interactions through a motor domain that lacks an active site. *Cell.* 128:1161–1172.

Arnal, I., and R.H. Wade. 1998. Nucleotide-dependent conformations of the kinesin dimer interacting with microtubules. *Structure.* 6:33–38.

Asbury, C.L. 2005. Kinesin: world's tiniest biped. *Curr. Opin. Cell Biol.* 17:89–97.

Asbury, C.L., A.N. Fehr, and S.M. Block. 2003. Kinesin moves by an asymmetric hand-over-hand mechanism. *Science.* 302:2130–2134.

Asenjo, A.B., N. Krohn, and H. Sosa. 2003. Configuration of the two kinesin motor domains during ATP hydrolysis. *Nat. Struct. Biol.* 10:836–842.

Asenjo, A.B., Y. Weinberg, and H. Sosa. 2006. Nucleotide binding and hydrolysis induces a disorder-order transition in the kinesin neck-linker region. *Nat. Struct. Mol. Biol.* 13:648–654.

Auerbach, S.D., and K.A. Johnson. 2005. Alternating site ATPase pathway of rat conventional kinesin. *J. Biol. Chem.* 280:37048–37060.

Berliner, E., E.C. Young, K. Anderson, H.K. Mahtani, and J. Gelles. 1995. Failure of a single-headed kinesin to track parallel to microtubule protofilaments. *Nature.* 373:718–721.

Boyer, P.D. 2002. Catalytic site occupancy during ATP synthase catalysis. *FEBS Lett.* 512:29–32.

Brady, S.T. 1985. A novel brain ATPase with properties expected for the fast axonal transport motor. *Nature.* 317:73–75.

Cohn, S.A., A.L. Ingold, and J.M. Scholey. 1989. Quantitative analysis of sea urchin egg kinesin-driven microtubule motility. *J. Biol. Chem.* 264:4290–4297.

Colquhoun, D., and F.J. Sigworth. 1995. Single-Channel Recording. 2nd ed. Plenum Press, NY. 489–560.

Coppin, C.M., J.T. Finer, J.A. Spudich, and R.D. Vale. 1996. Detection of sub-8-nm movements of kinesin by high-resolution optical-trap microscopy. *Proc. Natl. Acad. Sci. USA.* 93:1913–1917.

Crevel, I.M., A. Lockhart, and R.A. Cross. 1996. Weak and strong states of kinesin and ncd. *J. Mol. Biol.* 257:66–76.

Fersht, A. 1985. Enzyme structure and mechanism. 2nd ed. W.H. Freeman, New York. 117–118.

Gilbert, S.P., M.L. Moyer, and K.A. Johnson. 1998. Alternating site mechanism of the kinesin ATPase. *Biochemistry.* 37:792–799.

Guydosh, N.R., and S.M. Block. 2006. Backsteps induced by nucleotide analogs suggest the front head of kinesin is gated by strain. *Proc. Natl. Acad. Sci. USA.* 103:8054–8059.

Hackney, D.D. 1994. Evidence for alternating head catalysis by kinesin during microtubule-stimulated ATP hydrolysis. *Proc. Natl. Acad. Sci. USA.* 91:6865–6869.

Hancock, W.O., and J. Howard. 1998. Processivity of the motor protein kinesin requires two heads. *J. Cell Biol.* 140:1395–1405.

Hancock, W.O., and J. Howard. 1999. Kinesin's processivity results from mechanical and chemical coordination between the ATP hydrolysis cycles of the two motor domains. *Proc. Natl. Acad. Sci. USA.* 96:13147–13152.

Hirose, K., A. Lockhart, R.A. Cross, and L.A. Amos. 1995. Nucleotide-dependent angular change in kinesin motor domain bound to tubulin. *Nature.* 376:277–279.

Hoenger, A., M. Thormahlen, R. Diaz-Avalos, M. Doerhoefer, K.N. Goldie, J. Muller, and E. Mandelkow. 2000. A new look at the microtubule binding patterns of dimeric kinesins. *J. Mol. Biol.* 297:1087–1103.

Howard, J. 1997. Molecular motors: structural adaptations to cellular functions. *Nature.* 389:561–567.

Inoue, Y., A.H. Iwane, T. Miyai, E. Muto, and T. Yanagida. 2001. Motility of single one-headed kinesin molecules along microtubules. *Biophys. J.* 81:2838–2850.

Kaseda, K., H. Higuchi, and K. Hirose. 2002. Coordination of kinesin's two heads studied with mutant heterodimers. *Proc. Natl. Acad. Sci. USA.* 99:16058–16063.

Kaseda, K., H. Higuchi, and K. Hirose. 2003. Alternate fast and slow stepping of a heterodimeric kinesin molecule. *Nat. Cell Biol.* 5:1079–1082.

Kawaguchi, K., and S. Ishiwata. 2001. Nucleotide-dependent single- to double-headed binding of kinesin. *Science.* 291:667–669.

Kozielski, F., S. Sack, A. Marx, M. Thormahlen, E. Schonbrunn, V. Biou, A. Thompson, E.M. Mandelkow, and E. Mandelkow. 1997. The crystal structure of dimeric kinesin and implications for microtubule-dependent motility. *Cell.* 91:985–994.

Kuznetsov, S.A., and V.I. Gelfand. 1986. Bovine brain kinesin is a microtubule-activated ATPase. *Proc. Natl. Acad. Sci. USA.* 83:8530–8534.

Ma, Y.Z., and E.W. Taylor. 1997a. Interacting head mechanism of microtubule-kinesin ATPase. *J. Biol. Chem.* 272:724–730.

Ma, Y.Z., and E.W. Taylor. 1997b. Kinetic mechanism of a monomeric kinesin construct. *J. Biol. Chem.* 272:717–723.

Nishiyama, M., H. Higuchi, and T. Yanagida. 2002. Chemomechanical coupling of the forward and backward steps of single kinesin molecules. *Nat. Cell Biol.* 4:790–797.

Okada, Y., H. Yamazaki, Y. Sekine-Aizawa, and N. Hirokawa. 1995. The neuron-specific kinesin superfamily protein KIF1A is a unique monomeric motor for anterograde axonal transport of synaptic vesicle precursors. *Cell.* 81:769–780.

Rice, S., A.W. Lin, D. Safer, C.L. Hart, N. Naber, B.O. Carragher, S.M. Cain, E. Pechatnikova, E.M. Wilson-Kubalek, M. Whittaker, E. Pate, R. Cooke, E.W. Taylor, R.A. Milligan, and R.D. Vale. 1999. A structural change in the kinesin motor protein that drives motility. *Nature.* 402:778–784.

Rosenfeld, S.S., P.M. Fordyce, G.M. Jefferson, P.H. King, and S.M. Block. 2003. Stepping and stretching. How kinesin uses internal strain to walk processively. *J. Biol. Chem.* 278:18550–18556.

Schief, W.R., and J. Howard. 2001. Conformational changes during kinesin motility. *Curr. Opin. Cell Biol.* 13:19–28.

Schnapp, B.J., B. Crise, M.P. Sheetz, T.S. Reese, and S. Khan. 1990. Delayed start-up of kinesin-driven microtubule gliding following inhibition by adenosine 5′-[β,γ-imido]triphosphate. *Proc. Natl. Acad. Sci. USA.* 87:10053–10057.

Scholey, J.M., M.E. Porter, P.M. Grissom, and J.R. McIntosh. 1985. Identification of kinesin in sea urchin eggs, and evidence for its localization in the mitotic spindle. *Nature.* 318:483–486.

Uemura, S., K. Kawaguchi, J. Yajima, M. Edamatsu, Y.Y. Toyoshima, and S. Ishiwata. 2002. Kinesin-microtubule binding depends on both nucleotide state and loading direction. *Proc. Natl. Acad. Sci. USA.* 99:5977–5981.

Vale, R.D., T. Funatsu, D.W. Pierce, L. Romberg, Y. Harada, and T. Yanagida. 1996. Direct observation of single kinesin molecules moving along microtubules. *Nature.* 380:451–453.

Vale, R.D., T.S. Reese, and M.P. Sheetz. 1985. Identification of a novel force-generating protein, kinesin, involved in microtubule-based motility. *Cell.* 42:39–50.

Vugmeyster, Y., E. Berliner, and J. Gelles. 1998. Release of isolated single kinesin molecules from microtubules. *Biochemistry.* 37:747–757.

Yildiz, A., and P.R. Selvin. 2005. Kinesin: walking, crawling or sliding along? *Trends Cell Biol.* 15:112–120.

Young, E.C., H.K. Mahtani, and J. Gelles. 1998. One-headed kinesin derivatives move by a nonprocessive, low-duty ratio mechanism unlike that of two-headed kinesin. *Biochemistry.* 37:3467–3479.